Journal of Magnetics 13(4), 128-131 (2008)

Electronic Structures, Magnetic, and Superconducting Properties of bcc Ni and V-doped Ni ($Ni_{16-x}V_x$)

Bongjae Kim, Hong Chul Choi, Kyoo Kim, and B. I. Min*

PCTP, Department of Physics, Pohang University of Science and Technology, Pohang 790-784, Korea

(Received 7 November 2008, Received in final form 1 December 2008, Accepted 2 December 2008)

We have investigated the electronic structures and magnetic properties of both undoped and doped bcc Ni using the full-potential linearized augmented plane wave (FLAPW) band method. A ferromagnetic ground state is obtained at the equilibrium volume of bcc Ni. When the system is under strain, the nonmagnetic ground state is stabilized. When the Ni is doped with V, the $Ni_{16-x}V_x$ material loses its magnetic properties when $x > 2$. We have also discussed the possible superconducting properties of $Ni_{16-x}V_x$.

Keywords : electronic structure, bcc Ni, superconductor, V-doped Ni

1. Introduction

The crystal structure and the magnetic phase of a system are closely related. Considering that magnetism and superconductivity are generally completing, any structural change can generate superconductivity by suppressing magnetism. Typical magnetic transition metals, such as Fe, Co, and Ni, have been intensively studied to examine the correlation between structure and magnetism [1-4]. Note that ferromagnetic Fe, Co, and Ni have stable body-centered cubic (bcc), hexagonal close-packed (hcp), and face-centered cubic (fcc) structures, respectively. When an fcc structure of Fe is stabilized by growing epitaxially on a nonmagnetic Cu surface, the magnetic state has been changed to an antiferromagnetic spin density wave [5].

Artificially grown fcc Fe and bcc Co have been extensively studied, both experimentally and theoretically. However, bcc Ni has not been explored much due to its instability. From local spin density approximation (LSDA) band calculations, Moruzzi *et al.* [1, 2] found that the paramagnetic ground state of bcc Ni is stabilized. On the other hand, there have been reports that bcc Ni on an Fe substrate exhibits a non-vanishing magnetic moment [6, 7]. Since the substrate (Fe) itself is a magnetic material, the reliability of the magnetic moment value is reduced due to the effect of the magnetic coupling between the Fe and Ni. Recently, Tian *et al.* [8] successfully fabricated bcc Ni on GaAs and measured the magnetic moment with much improved precision (0.52 μ_B/atom). The results indicated a ferromagnetic ground state for bcc Ni. Subsequent *ab-initio* band calculations yielded similar results [9-11].

Aside from the issue of the magnetic ground state, bcc Ni is interesting due to its possible very weak itinerant ferromagnetic nature [10] and its reduced Curie temperature compared to fcc Ni [11]. In this study, we have reexamined the electronic and magnetic properties of bcc Ni and its transition from a ferromagnetic to a paramagnetic phase upon varying its lattice constant. Furthermore, we have investigated the electronic structures and magnetic properties of vanadium (V)-doped Ni ($Ni_{16-x}V_x$). The vanadium is added to stabilize the bcc Ni structure. The possible superconducting properties of bcc $Ni_{16-x}V_x$ have also been discussed.

2. Results and Discussion

We have employed the full-potential linearized augmented plane wave (FLAPW) band method [12]. For the exchange-correlation energy, we employed the generalized gradient approximation (GGA) [13].

2.1. Bulk bcc Ni

For the bulk bcc Ni, a ferromagnetic ground state has been found at the calculated equilibrium lattice constant of 2.785 Å with a magnetic moment of 0.528 μ_B/atom.

*Corresponding author: Tel: +82-54-279-2074
Fax: +82-54-279-3099, e-mail: bimin@postech.ac.kr

This is in good agreement with both previous experimental and band calculation results. One thing to note here is that the calculated equilibrium lattice constant of bulk bcc Ni is smaller than the real (experimental) lattice constant of a bcc Ni film grown on GaAs (2.82 Å) [8]. This implies that the bcc Ni film grown on GaAs is under tensile strain. A body-centered-tetragonal (bct) structure can be established due to this lattice mismatch. The c/a ratio, however, is not much different from one. Thus, it is expected that the magnetic behavior of bct Ni is not significantly different from that of bcc Ni, making the bcc calculation valid [10].

The actual magnetic moment at the calculated equilibrium lattice constant is considered to be slightly different from the experimental value since the volume of the bcc Ni plays a key role in determining the magnetic stability. This can be seen in Fig. 1(a). The lattice constants of bulk bcc Ni and a bcc Ni film grown on GaAs are marked with dotted lines. As the lattice parameter of the bcc Ni reduces, the energy difference between the ferromagnetic and paramagnetic states becomes negligible. The bcc Ni film grown on GaAs has a larger lattice constant than the bulk bcc Ni. Therefore, the stability of the magnetism will be stronger for the bcc Ni film. Fig. 1(b) shows the dependence of the magnetic moment on the lattice parameter of the bulk bcc Ni. As the volume decreases, or

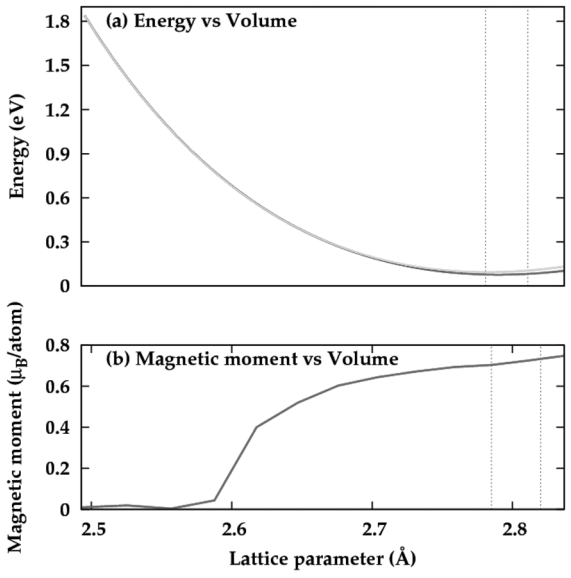

Fig. 1. (a) Total energy vs. lattice parameter for the bulk bcc Ni. The ferromagnetic state is stabilized at the equilibrium lattice parameter. At reduced volume, the paramagnetic state is stabilized. (b) Magnetic moment vs. lattice parameter. The paramagnetic behavior emerges with decreasing the lattice parameter. The lattice parameters of the bulk bcc Ni and the Ni film grown on GaAs are marked with dotted lines.

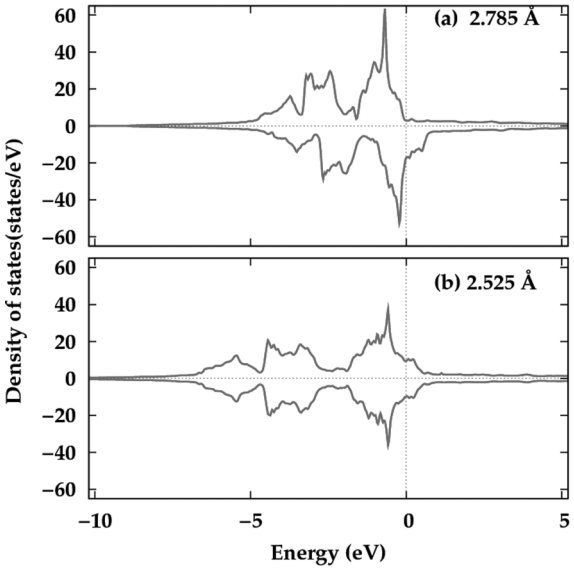

Fig. 2. DOS of the bulk bcc Ni. (a) DOS at the equilibrium lattice parameter, a=2.785 Å. (b) DOS at the reduced lattice parameter, a=2.525 Å. Note that both DOS correspond to a 16-atom supercell.

the pressure increases, the magnetic moment of the bcc Ni decreases. If the lattice constant is reduced to less than 2.6 Å, the magnetism of the bcc Ni disappears and a paramagnetic phase emerges.

In Fig. 2, the density of states (DOS) of bcc Ni is shown with the Fermi energy at zero. The DOS at the calculated equilibrium lattice constant in Fig. 2(a) shows clear ferromagnetic behavior. When the volume is compressed, the DOS exhibits nonmagnetic behavior at the lattice constant of 2.525 Å, as shown in Fig. 2(b).

2.2. V-doped Ni ($Ni_{16-x}V_x$ (x = 1, 2, 3, and 4))

Natural Ni has an fcc structure. So, even though bcc Ni can be produced, its stability is rather low. Doping bulk bcc Ni with another bcc element, such as V or Cr, may reinforce the bcc character of Ni. Therefore, we examined the effect of doping with V. To do this, we considered a supercell of bcc Ni in which some of the Ni atoms had been replaced by V atoms, as shown in Fig. 3.

Doping with V has a tendency to suppress the magnetism. Fig. 4 shows the magnetic moment as a function of the volume for bcc Ni, $Ni_{15}V$, $Ni_{14}V_2$, $Ni_{13}V_3$, and $Ni_{12}V_4$. The equilibrium lattice parameter is slightly increased from 2.785 to 2.811 Å due to the larger lattice constant of 3.02 Å for bcc V [14]. It is clear that replacing 1/16 of the Ni atoms with V atoms ($Ni_{15}V$) greatly reduces the magnetic moment. At the equilibrium volume of $Ni_{15}V$, the magnetic moment is 0.309 μ_B/atom. This is more than 40% lower than the value (0.544 μ_B/atom)

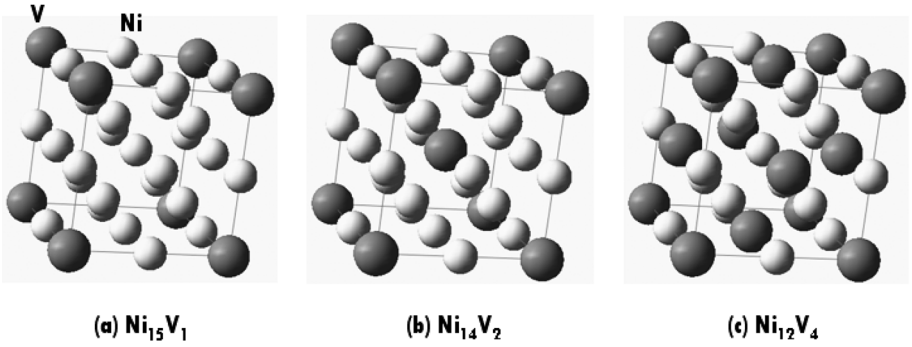

Fig. 3. The structures of the three V-doped Ni materials. (a) $Ni_{15}V_1$, (b) $Ni_{14}V_2$, and (c) $Ni_{12}V_4$.

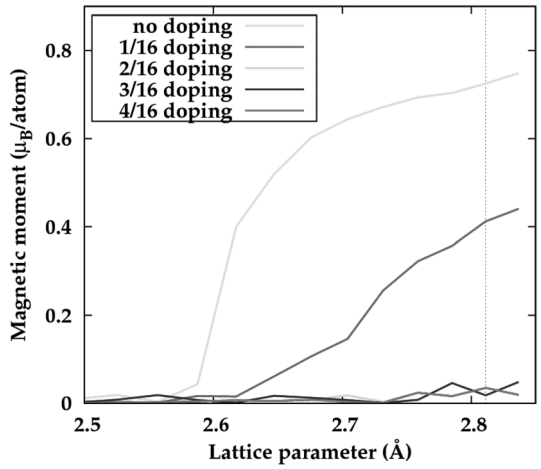

Fig. 4. Magnetic moment vs. lattice parameter for $Ni_{16-x}V_x$ (x = 0, 1, 2, 3, and 4). The equilibrium lattice parameter, a=2.811 Å, is marked with a dotted line.

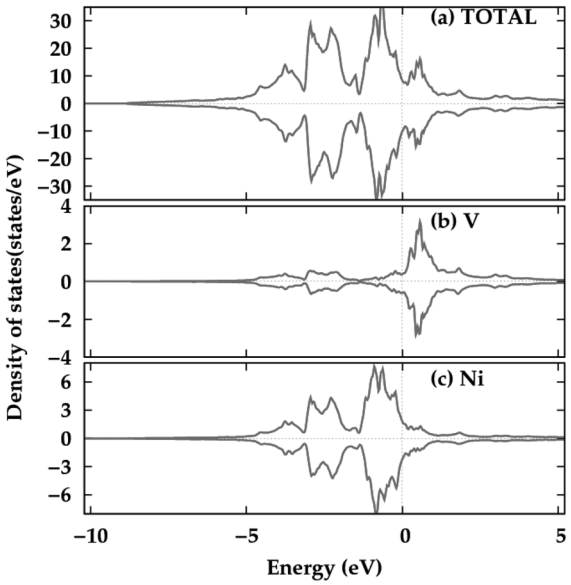

Fig. 5. Total and local DOS for $Ni_{14}V_2$ at the equilibrium lattice parameter. (a) Total DOS, (b) local DOS of V, and (c) local DOS of Ni.

obtained for the bulk bcc Ni. As the lattice constant decreases, the magnetic moment of $Ni_{15}V$ is reduced much faster than that of the bulk bcc Ni. This means that the magnetic moment of $Ni_{15}V$ is soon less than half that of the bulk bcc Ni at the same lattice parameter. $Ni_{15}V$ changes into a paramagnetic ground state at about 2.62 Å. According to Fig. 4, at this lattice constant, the bulk bcc Ni still has a large magnetic moment.

If more than 2/16 of the Ni atoms are replaced by V atoms, the magnetic moment vanishes and the paramagnetic ground state is stabilized even at the equilibrium lattice parameter. Fig. 4 shows that the magnetic moments vanish for all three lattice compositions ($Ni_{14}V_2$, $Ni_{13}V_3$, and $Ni_{12}V_4$). In Fig. 5, the total and local DOS for $Ni_{14}V_2$ are given at its equilibrium lattice constant. It is clear that the hybridization between the Ni and V states is strong. This hybridization would lead to the suppression of magnetism in $Ni_{14}V_2$. Therefore, one can conclude that doping with V suppresses the magnetism of bcc Ni. This is similar to applying pressure to bulk bcc Ni.

2.3. Superconducting properties of $Ni_{16-x}V_x$

Using McMillan's formula [15] based on the linearized muffin-tin orbital (LMTO) band results, we have examined the possible superconducting properties of the bcc stabilized $Ni_{16-x}V_x$ materials. In McMillan's formula, the superconducting transition temperature T_c is given by

$$T_c = \frac{\Theta_D}{1.45}\exp\left\{\frac{-1.04(1+\lambda+\mu_{sp})}{\lambda-(\mu+\mu_{sp})(1+0.62\lambda)}\right\}$$

Here, Θ_D is the Debye temperature, λ is the electron-phonon coupling constant, μ is the effective electron-electron interaction parameter, which we set as 0.13, and μ_{sp} is the spin fluctuation parameter, which we set equal to zero. The electron-phonon coupling constant can be obtained by $\lambda = \sum_{\alpha} \eta_\alpha / M_\alpha \langle \omega_\alpha^2 \rangle$, where η_α is a superconducting parameter for each element and is defined as

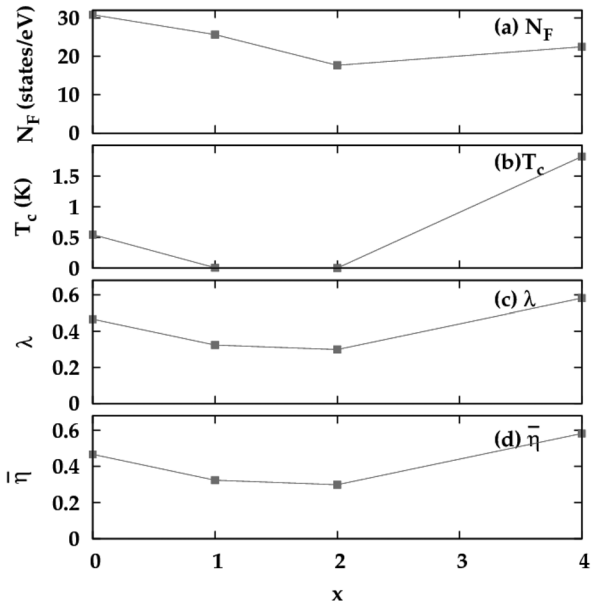

Fig. 6. Superconducting properties of the $Ni_{16-x}V_x$ (x = 0, 1, 2, and 4) materials at their equilibrium lattice parameters. (a) DOS at the Fermi energy, (b) superconducting transition temperature T_c, (c) electron-phonon coupling constant λ, and (d) averaged superconducting parameter $\bar{\eta}$.

$\eta_\alpha = N_F \langle I_\alpha^2 \rangle$. Here, N_F is the DOS at the Fermi energy and $\langle I_\alpha^2 \rangle$ is the average electron-ion interaction matrix element for the α-th ion. $\langle \omega_\alpha^2 \rangle$ corresponds to the average phonon frequency squared for the α-th ion. $\langle I_\alpha^2 \rangle$ can be determined from the band structure results by using the rigid muffin-tin approximation [16]. We estimated the $\langle \omega_\alpha^2 \rangle$ of Ni from that of bcc Fe by accounting for the mass difference between Fe and Ni.

Fig. 6 displays the changes in N_F, T_c, λ, and $\bar{\eta}$ for $Ni_{16-x}V_x$ upon varying x between 0, 1, 2, and 4. Note that since η_α is different for each atom, the average value ($\bar{\eta}$) is shown instead. It is clear that with increasing V, the superconducting tendency seems to initially decrease: both λ and $\bar{\eta}$ are reduced so that T_c goes to almost zero. However, the superconducting character of $Ni_{12}V_4$ seems to emerge rapidly. Both λ and $\bar{\eta}$ increase to produce a higher T_c.

3. Conclusions

We have investigated the electronic structures and magnetic properties of bcc Ni and V-doped Ni ($Ni_{16-x}V_x$). For the bulk bcc Ni, a ferromagnetic ground state is obtained at the equilibrium volume. However, the magnetism disappears upon applying pressure. When bcc Ni is doped with V, the magnetism is greatly reduced. If more than 2/16 of the Ni atoms are replaced by V atoms, the magnetic moment vanishes and the paramagnetic ground state is stabilized at the equilibrium lattice parameter.

Regarding the superconducting properties of the bcc stabilized $Ni_{16-x}V_x$, we can see that when the V doping content is small, even though magnetism is suppressed, the superconducting behavior is weakened first with increasing x, but becomes strengthened for x = 4. Our study therefore suggests that superconductivity in bcc-type Ni systems can be realized either by compressing bulk bcc Ni or by doping it with more than 25% of V.

Acknowledgments

This work was supported by the POSTECH BK21 Physics Division.

References

[1] V. L. Moruzzi, Phys. Rev. Lett. **57**, 2211 (1986).
[2] V. L. Moruzzi, P. M. Marcus, and J. Kubler, Phys. Rev. B **34**, 1784 (1986).
[3] B. I. Min, T. Oguchi and A. J. Freeman, Phys. Rev. B **33**, 7852 (1986).
[4] J. I. Lee, Soon C. Hong, and A. J. Freeman, Phys. Rev. B **47**, 810 (1993).
[5] D. Qian, X. F. Jin, J. Barthel, M. Klaua, and J. Kirschner, Phys. Rev. Lett. **87**, 227204 (2001).
[6] J. A. C. Bland, R. D. Bateson, A. D. Johnson, B. Heinrich, Z. Celinski and H. J. Hauter, J. Magn. Magn. Mater. **93**, 331 (1991).
[7] N. B. Brookes, A. Clarke, and P. D. Johnson, Phys. Rev. B **46**, 237 (1992).
[8] C. S. Tian, D. Qian, D. Wu, R. H. He, Y. Z. Wu, W. X. Tang, L. F. Yin, Y. S. Shi, G. S. Dong, X. F. Jin, X. M. Jiang, F. Q. Liu, H. J. Qian, K. Sun, L. M. Wang, G. Rossi, Z. Q. Qiu, and J. Shi, Phys. Rev. Lett. **94**, 137210 (2005).
[9] G. Y. Guo, and H. H. Wang, Chin. J. Phys. (Taipei) **38**, 949 (2000).
[10] S. Khmelevskyi and P. Mohn, Phys. Rev. B **75**, 012411 (2007).
[11] P. Yu, X. F. Jin, J. Kudrnovsky, D. S. Wang, and P. Bruno, Phys. Rev. B **77**, 054431 (2008).
[12] M. Weinert, E. Wimmer, and A. J. Freeman, Phys. Rev. B **26**, 4571 (1982); H. J. F. Jansen and A. J. Freeman *ibid.* **30**, 561 (1984).
[13] J. P. Perdew, K. Burke, and M. Ernzerhof, Phys. Rev. Lett. **77**, 3865 (1996).
[14] N. W. Ashcroft and N. D. Mermin, Solid State Physics, Thomson Learning (1976).
[15] W. L. McMillan, Phys. Rev. **167**, 331 (1968).
[16] G. D. Gaspari and B. L. Gyorffy, Phys. Rev. Lett. **28**, 801 (1972).